

Interactive Multiple Model Sensor Analysis for Unmanned Aircraft Systems (UAS) Detect and Avoid (DAA)

Adriano Canolla, Michael B. Jamoom, Boris Pervan

Department of Mechanical, Materials
and Aerospace Engineering
Illinois Institute of Technology
Chicago, IL 60616

Email: acanolla@hawk.iit.edu, mjamoom@iit.edu, pervan@iit.edu

Abstract—This research aims at improving Detect and Avoid (DAA) functions in Unmanned Aircraft Systems (UAS) using a Multiple Model Estimation algorithm to track maneuvering intruders. This research builds on previous work that used predefined aircraft encounter trajectories. An established encounter model generates the intruder trajectories while a multiple model algorithm is introduced to improve intruder dynamics estimation. A new method based on the Kalman prediction phase inside the Interactive Multiple Model (IMM) algorithm is presented to estimate time to closest point of approach, horizontal miss distance, and vertical separation. An analysis of the sensor error on the algorithm estimation and the sensor field of regard requirement from the Air-to-Air Radar Minimum Operational Performance Standards (MOPS) is performed. The efficiency of the trajectory estimation has direct implication on the estimation of the intruder trajectory in relation to the own aircraft. The methods described in this research can aid a certification authority in determining if a DAA system is sufficient for safely integration of UAS into the National Airspace System.

I. INTRODUCTION

This research describes new methods to apply safety standards in Detect and Avoid (DAA) functions for Unmanned Aircraft Systems (UAS) using target tracking and encounter models. With the expanding range of applications for UAS operations, the United States Congress mandated the Federal Aviation Administration (FAA), through the FAA Modernization and Reform Act of 2012, to develop necessary requirements for integration of UAS into the National Airspace System [1]. While a manned aircraft’s pilot relies on human vision to see and avoid non-cooperative intruders (those not employing a transponder or Automatic Dependent Surveillance-Broadcast, ADS-B) [2], a UAS requires sensors to Detect and Avoid intruder aircraft to ensure that safety targets are met.

Previous work used predefined linear encounter trajectories (either with constant velocity or linear acceleration) for the sensor uncertainty analysis, focusing on potential borderline cases as a test for the methodology [3]. This research improves the intruder dynamics estimation using the Multiple Model Adaptive Estimation (MMAE) concept to track the maneuvering intruder aircraft [4][5], using an established encounter model to generate the intruder trajectories. This better accounts

for the likelihood of different types of encounters and include potential worst-case intruder trajectories. In addition to the other estimation error sources presented in previous work [4], we further investigate the sensor noise using a typical sensor from the Minimum Operational Performance Standards (MOPS) [6] and also the effect of the field of regard requirements. This research serves as a continuation effort to evaluate the MMAE tracking applied to realistic trajectories on the UAS DAA capabilities for realistic intruder encounters.

A. Well Clear

Since a UAS will not have a pilot on board, it will have to replace pilot vision functionality through appropriate sensors. DAA sensors include radar, Laser/Light Detection and Ranging (LIDAR), Electro-Optical (EO), acoustic, and Infrared (IR) [7], [8]. Until 2014, the self-separation (SS) concept of keeping aircraft well clear of each other had never been fully defined, despite “well clear” being a widely recognized term by the FAA and International Civil Aviation Organization (ICAO) [9]. Recently, the Radio Technical Commission for Aeronautics (RTCA) Special Committee-228 (SC-228), in their Phase I Detect and Avoid (DAA) Minimum Operational Performance Standards (MOPS), defined a Loss of Well Clear (LoWC), which can also be considered a Well Clear Threshold (WCT), as the time to horizontal closest point of approach (CPA), or τ , of 35 seconds, a horizontal miss distance (HMD) of 4000 ft, and a vertical miss distance of 450 ft [6]. In this paper, we consider τ , HMD, and vertical miss distance to be “hazard states,” which define the hazard of a loss of well clear between two aircraft.

When an intruder cannot remain well clear, a collision avoidance maneuver is required to avoid a near mid-air collision (NMAC). NMAC limits are defined as 500 ft laterally and 100 ft vertically from the own aircraft [10] and are shown, along with the WCT and CPA, in Figure 1.

This work employs WCT and self-separation limits, although the same methodology could be applied to NMAC and collision avoidance limits.

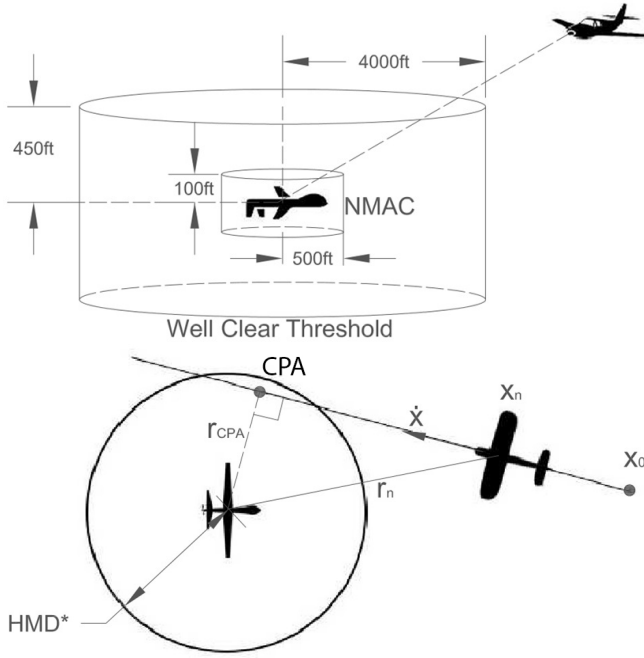


Fig. 1: Well Clear Threshold, CPA, and NMAC

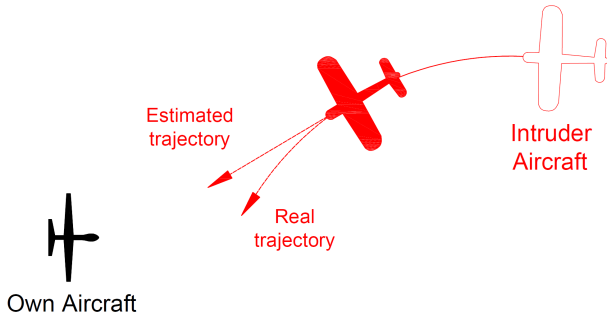


Fig. 2: Intruder aircraft tracking

B. Target Tracking

The DAA system of the UAS (the own aircraft) must detect a non-cooperative intruder aircraft (a target), then estimate its trajectory. Uncertainty in the measurement due to sensor noise will give poor state estimates when the intruder is first detected by the sensors, but as the DAA system gets more sensor measurements, the estimation error decreases. Adding to the measurement uncertainty, when tracking maneuvering intruders (with nonlinear trajectories), there is no knowledge of changes in intruder behavior [11]. A standard Kalman filter (KF) solution with a single motion model present limited performance for such problems due to the dynamics changes as the target maneuvers. For this situation, state estimation can be improved using Multiple Model Adaptive Estimation (MMAE) to account for different potential intruder behaviors [12].

1) *Multiple Model Adaptive Estimation*: MMAE assumes that the target dynamic model is one of a discrete set of r models [12]. These filters all run in parallel to estimate the

states of targets with changing dynamics. The probabilities of switching from one model to any other model in the next epoch are cataloged in a Markov Chain transition probability matrix, which characterize potential mode transitions. These systems are called hybrid since they have both continuous (noise) and discrete (mode or model) uncertainties [12].

2) *IMM Algorithm*: The optimal approach to filtering the states of a multiple model system requires running filters for every possible model sequence. That is, for r models, r^k optimal filters must be implemented to process measurements at time step k , being computationally unfeasible for our application. In practical applications of multiple model systems, one of the popular practical algorithms for the MMAE is the Interacting Multiple Model (IMM) estimator. The IMM estimator is a suboptimal hybrid filter that has been shown to achieve an excellent compromise between performance and complexity [13], [14], whose model changes according to a finite-state, discrete-time Markov Chain [12], [15]. In the IMM, each state estimate is computed under each possible current (time step t) model using r filters, with each filter using a different combination of the previous (time step $t-1$) model-conditioned estimates (which are the mixed initial conditions). The regime switching is usually modeled by a finite state homogeneous Markov Chain, with a-priori known transition probabilities. This algorithm can be divided into five stages: (1) calculation of mixing probabilities, (2) mixed initial states and covariances, (3) filtering, (4) mode probability update and (5) state estimate combination (output only, stage five is not part of the recursion). A flowchart of the IMM algorithm is depicted in Figure 3:

where:

- $\mathbf{x}_n(k-1|k-1)$ and $\mathbf{P}_n(k-1|k-1)$ are the previous states and covariances, at time step $k-1$, for each individual mode n .
- $\mathbf{x}_{nm}(k-1|k-1)$ and $\mathbf{P}_{nm}(k-1|k-1)$ are the mixed states and covariances, at time step $k-1$, for each individual mode n .
- $\mathbf{x}_n(k|k)$ and $\mathbf{P}_n(k|k)$ are the calculated states and covariances, at time step k , for each individual mode n .
- $\mathbf{x}(k|k)$ and $\mathbf{P}(k|k)$ are the combined states and covariances, at time step k .
- $\mu(k)$ is the mode probability at time step k .
- $\mu(k|k)$ is the mixing probability at time step k .
- $\Lambda(k)$ is the likelihood function at time step k .
- $\mathbf{z}(k)$ is the DAA sensor measurement at time step k .

C. Contributions of this Research

The main research goal is (1) to develop new methods for the UAS DAA system, addressing the system safety performance with a maneuvering intruder and (2) developing a new method for hazard state estimation, advancing previous work that used predefined, linear trajectories [4][16]. We generate random trajectories using an established encounter model to account for realistic trajectories and apply intruder tracking using a Multiple Model Adaptive Estimation (MMAE) algorithm. The algorithm chosen was the Interactive Multiple

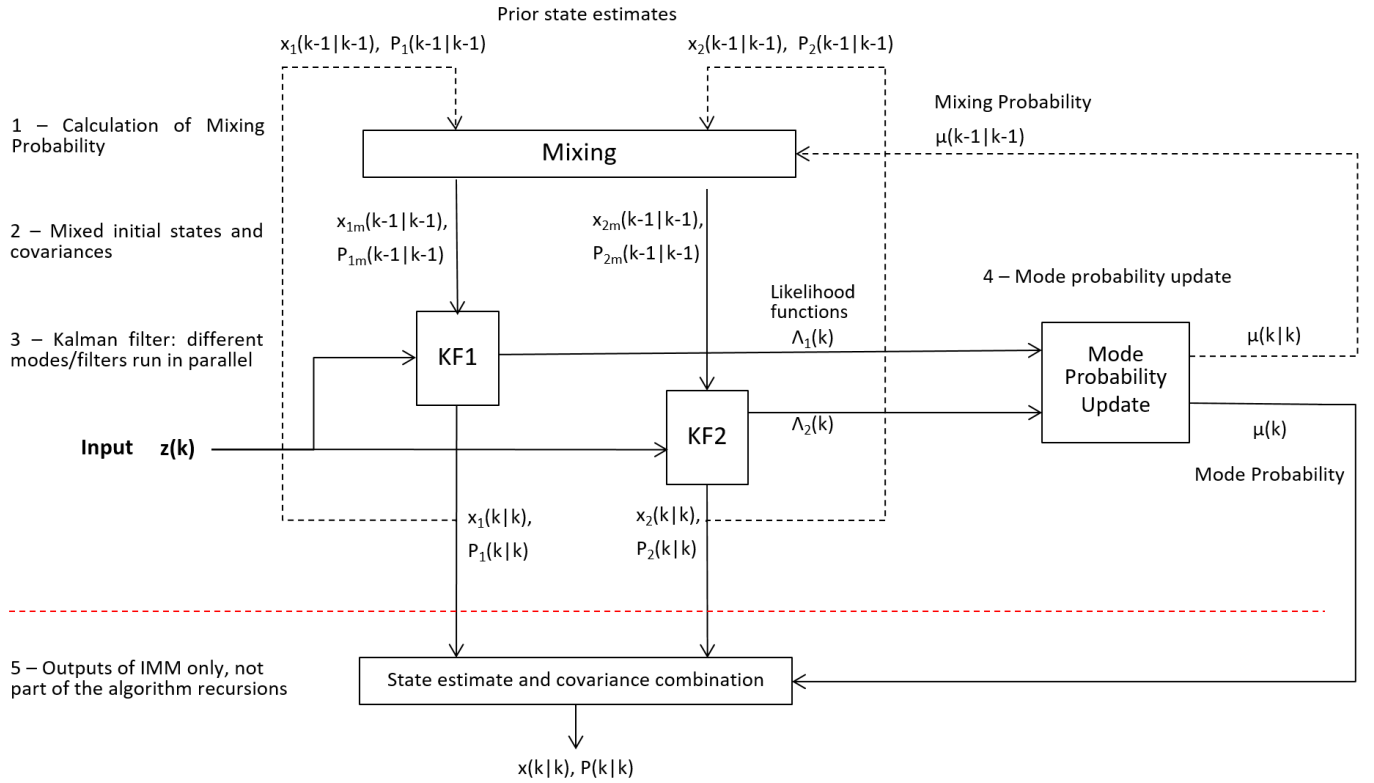


Fig. 3: IMM Algorithm

Model (IMM). In previous work, we demonstrated the IMM performance comparing it with the Perfect IMM, which is used as a benchmark for the mode adaptation analysis [4]. Also in previous work, we developed a new method for estimating hazard states to account for the maneuvering intruders, since the DAA MOPS only consider a linear, non-accelerated trajectory [6]. In this work, in order to fully account for all the different error sources we identify, we analyze the IMM general methodology performance against a realistic sensor as given in the Air-to-Air MOPS [6]. Also, we add the field of regard requirements as presented in the Air-to-Air Radar MOPS [17].

D. Paper Outline

After this introductory section, the second section introduces the methodology of the multiple model estimation method, the new method for the hazard state estimation, the problem formulation and the Interactive Multiple Model algorithm (IMM) selected among the MMAE algorithms for this work. The third section presents analysis for a particular trajectory and for a Monte Carlo analysis of likely trajectories. The final section provides conclusions and opportunities for future research.

II. METHODOLOGY

In this section, we present the methodology behind the IMM algorithm, starting from the Kalman Filters that correspond to each individual IMM mode. Following the formal definition

of the hazard state, we present the methodology behind the new method for the hazard state estimation.

A. Relative Intruder State

Each state space model can be expressed with equations of the following form:

$$\mathbf{x}_k = \mathbf{F}_{k-1}\mathbf{x}_{k-1} + \mathbf{G}_{k-1}\mathbf{u}_{k-1} + \mathbf{q}_{k-1} \quad (1)$$

$$\mathbf{z}_k = \mathbf{H}_k\mathbf{x}_k + \mathbf{r}_k \quad (2)$$

where:

- $\mathbf{x}_k \in R^n$ are the system states (intruder Cartesian position, velocity, and acceleration in inertial coordinates) at time step k .
- \mathbf{F}_{k-1} is the transition matrix of the dynamic model.
- \mathbf{G}_{k-1} is the transition matrix of the dynamics of the own aircraft.
- \mathbf{u}_{k-1} are the own aircraft states in inertial coordinates.
- $\mathbf{q}_{k-1} \sim N(0; \mathbf{Q}_{k-1})$ is the process noise at time step $k-1$.
- $\mathbf{z}_k \in R^m$ is the cartesian relative intruder measurement at time step k .
- \mathbf{H}_k is the measurement model matrix.
- $\mathbf{r}_k \sim N(0; \mathbf{R}_k)$ is the measurement (sensor) noise on time step k .
- The initial distribution for the state is $\mathbf{x}_0 \sim N(0; \hat{\mathbf{P}}_0)$, where $\hat{\mathbf{P}}_0$ is typically large based on the lack of initial knowledge about the target.

where the matrices \mathbf{F}_a and \mathbf{F}_b are:

$$\mathbf{F}_a = \begin{bmatrix} 1 & \frac{\sin(\omega T)}{\omega} & \frac{(1-\cos(\omega T))}{(\omega^2)} \\ 0 & \cos(\omega T) & \frac{\sin(\omega T)}{\omega} \\ 0 & -\omega \sin(\omega T) & \cos(\omega T) \end{bmatrix} \quad (14)$$

$$\mathbf{F}_b = \begin{bmatrix} 1 & T & 0 \\ 0 & 1 & 0 \\ 0 & 0 & 0 \end{bmatrix} \quad (15)$$

$$\mathbf{G} = \mathbf{F}^I - \mathbf{F}^O \quad (16)$$

where T is the simulation time step.

$$\mathbf{u} = [0 \quad \dot{x}_{own} \quad 0 \quad 0 \quad \dot{y}_{own} \quad 0 \quad 0 \quad \dot{z}_{own} \quad 0]^T \quad (17)$$

where \dot{x}_{own} , \dot{y}_{own} and \dot{z}_{own} are the own aircraft velocity components. Here, we have assumed that our own aircraft has a constant velocity vector during the encounter. Strictly, this assumption is not necessary at this point in the general development. However, we write it here as an example because we will use it the performance analysis later in the paper.

Then the turning rate ω is defined by:

$$\omega = \frac{\|\mathbf{a}\|}{\|\mathbf{v}\|} = \frac{\sqrt{\ddot{x}^2 + \ddot{y}^2 + \ddot{z}^2}}{\sqrt{\dot{x}^2 + \dot{y}^2 + \dot{z}^2}} \quad (18)$$

where \mathbf{a} and \mathbf{v} are the accelerations and velocity vectors, in the inertial frame.

Considering the case where we have only relative position measurements, for example, the measurement matrix is:

$$\mathbf{H} = \begin{bmatrix} 1 & 0 & 0 & 0 & 0 & 0 & 0 & 0 & 0 \\ 0 & 0 & 0 & 1 & 0 & 0 & 0 & 0 & 0 \\ 0 & 0 & 0 & 0 & 0 & 0 & 1 & 0 & 0 \end{bmatrix} \quad (19)$$

The matrices for the other modes are similarly defined, and can be seen in details in [5].

3) *Transition Matrix Probabilities*: The IMM estimator assumes that the Transition Matrix of the Markov Chain governing the mode jumps is known. However, it is very difficult to determine the appropriate matrix quantities and identify a Markov transition law that optimally fits the unknown target motion [15].

Fortunately, we used the MIT Lincoln Lab Encounter Model itself, which is based on radar observations [18] to get the best available mode transition matrix. To do this, we ran the encounter model 10^6 times and recorded each mode transition, in order to get the likelihood of all mode changes during the encounters. We used these runs to build the Transition Matrix, as detailed in [5].

C. Hazard States

The DAA MOPS introduces the term DAA Well Clear (DWC) as ‘‘a temporal and/or spatial boundary around the aircraft intended to be an electronic means of avoiding conflicting traffic’’ [6]. DWC is synonymous with the WCT. The MOPS mathematically defines DWC in the following equation for a Loss of DWC (LoWC):

$$LoWC = [0 \leq \tau_{mod} \leq \tau_{mod}^*] \quad \text{and} \quad [HMD \leq HMD^*] \quad \text{and} \quad [-h \leq d_h \leq h^*] \quad (20)$$

with $\tau_{mod}^* = 35sec$, $HMD^* = 4000ft$ and $h^* = 450ft$.

The DAA MOPS LoWC threshold is synonymous with the WCT. Based on the DAA MOPS, these variables, or hazard states, are:

- Horizontal CPA or HMD
- Modified Tau (τ_{mod})
- Vertical Separation (h)

There are two ways to determine the HMD. One is the time based definition in the DAA MOPS and the other is geometrically determined based on a linear intruder trajectory. The geometric HMD can be derived from the definition [19] and its expression is:

$$HMD = \frac{\dot{y}x - \dot{x}y}{\sqrt{\dot{x}^2 + \dot{y}^2}} \quad (21)$$

The hazard states define the LoWC, which happens when all three are below their thresholds. The previous analysis [4] was done using the DAA MOPS formulas, for HMD and τ_{mod} [6]:

$$HMD = \sqrt{(d_x + v_{rx}t_{CPA})^2 + (d_y + v_{ry}t_{CPA})^2} \quad (22)$$

$$\tau_{mod} = \max(0, -\frac{d_x v_{rx} + d_y v_{ry}}{v_{rx}^2 + v_{ry}^2}) \quad (23)$$

where:

- $v_{rx} = \dot{x}_2 - \dot{x}_1$ is the relative horizontal velocity in the x direction
- $v_{ry} = \dot{y}_2 - \dot{y}_1$ is the relative horizontal velocity in the y direction
- $d_x = x_2 - x_1$ is the current horizontal separation on the x direction
- $d_y = y_2 - y_1$ is the current horizontal separation on the y direction

The vertical separation for alerting performance requirements are based on actual altitudes of the own and intruder aircrafts. We assume constant vertical velocity to account for the lookahead time alert criteria. These MOPS equations for the hazard states are based upon a linear trajectory with constant velocity being extended in the future. As will be explained in Section II-E, a linear trajectory can be a problematic approximation for a nonlinear trajectory.

D. IMM Estimation Error Sources

The IMM algorithm has estimation errors that are not directly related with its calculated covariances. The total error in the hazard states and trajectory prediction will be a sum of different error sources. Some will depend on the quality of the implementation of the algorithm, others on the inherently noisy measurements from the DAA system. In summary, we can divide the main contributors of the error into four parts:

- **Modeling error:** This is partly due to the modeling errors, where a maneuver, by its nature, does not follow the assumptions of the standard dynamic models used in the IMM [14].
- **Sensor noise:** Random noise on the sensor measurements.
- **Mode transition:** A relatively large estimation error is needed for the algorithm to recognize sudden changes in system modes, i.e. the adaptation might not be rapid enough. In previous work, we investigated this error through a performance comparison analysis with the Perfect IMM, in which the true mode of the target is known [4].
- **Prediction error:** Since our analysis covers maneuver changes along the simulation and we cannot predict future intruder intent, we have an additional source of error which consists of the prediction error of the estimated hazard states (in Section II-C) from the actual hazard states, which is only known after an encounter has ended.

In a real IMM, even with perfect measurements, we would still have uncertainty in trajectory estimation due to the approximate motion models used.

E. New Hazard States Estimation Method

To minimize prediction errors on the hazard states, we introduce a new method instead of using the linear trajectory approximation. The approach is to use the IMM prediction in the Kalman prediction step as the estimation for the hazard states. We now have four different ways to define the hazard states:

- **MOPS:** using the formulas as defined by the DAA MOPS in Equation (22) and *true trajectory data*.
- **IMM-MOPS:** using the formulas as defined by the DAA MOPS in Equation (22) and the best IMM trajectory estimation.
- **IMM-Predicted:** the estimated hazard states calculated at each time step, using the new IMM prediction method for extending the future trajectory.
- **True:** only known after the encounter is completed (influenced by future mode switches).

The method can be used to estimate any of the defined hazard states, but as an example, we examine the CPA/HMD since it is more affected by the maneuvering trajectories. It is interesting to note that the difference between MOPS CPA and IMM-MOPS CPA is only due to estimation errors in the IMM estimation, since both use the same method. While an estimated CPA was valid for a particular epoch, future maneuver changes (unknown to the own aircraft) result in

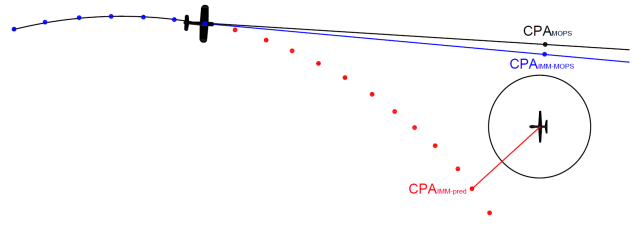


Fig. 4: CPA estimation

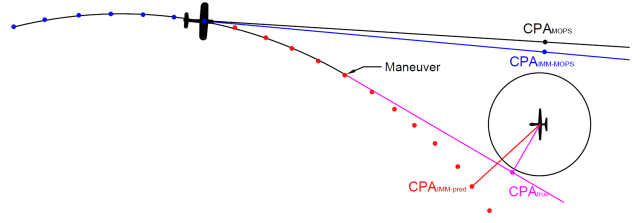


Fig. 5: Future maneuver change

changes to the True CPA, so the True CPA can only be known after an encounter is completed. The True CPA is an analysis tool, to be used for benchmark comparisons of these prediction methods.

An example of the MOPS, IMM-MOPS, and IMM-Predicted CPAs are depicted in Figure 4. The difference between CPA_{MOPS} and $CPA_{IMM-MOPS}$ is due to the error in the IMM state estimation when compared to the true trajectory and states. The new CPA estimation method is shown as $CPA_{IMM-PRED}$. Under maneuvers, the hazard state estimation will be changing at each time step.

Using the knowledge of the current maneuver can improve our estimation based on the IMM prediction. After a maneuver occurrence in the future (as shown in Figure 5), the new estimation gets better as the IMM recognizes the maneuver and adjusts for a new prediction subsequently.

We should note that, even though the focus on the representation is on the CPA, τ and vertical separation can also be extracted using the same method. We chose the CPA since it is easier to visualize graphically and also it represents the greater change in the calculation between the new method and the linear formula.

III. ANALYSIS

A. Field of Regard

According to the Air-to-Air MOPS, sensors should be able to identify targets within the following field of regard (FOR) [17]:

- $\pm 110^\circ$ with respect to the longitudinal axis
- $\pm 15^\circ$ vertically referenced to the flight path

Considering that the preliminary results were using 360 degrees, and most of the worst-case scenarios found were from trajectories that the intruder was overtaking the own aircraft from behind, we expect improvement on the estimation errors.

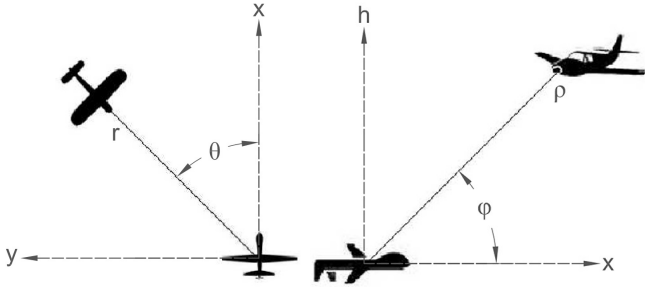


Fig. 6: Spherical sensor measurements

Also, an analysis of the likelihood of overtaking encounters can be made using the data from the Encounter Model, to analyze the relevance or not of these FOR values. Due to the field of regard requirements from the MOPS, some encounters previously generated will have the intruder Aircraft lying outside of the FOR from the onset of the encounter. In order to adapt for the FOR requirements, we defined new requirements for the intruder aircraft at its random initial position at the encounter cylinder

B. Sensor Noise

The DAA sensors measure (with an associated error) the intruder relative position in spherical coordinates. Taking from the DAA MOPS, these input measurements from a DAA radar includes relative slant range, relative range rate, relative bearing, and elevation angle. In our sensor measurement model we assume intruder spherical measurement vectors of range, azimuth angle and elevation angle, as in Figure 6.

According to the typical nominal non-cooperative DAA sensor measurements, the composite nominal sensor will have the following typical accuracy values [17][19]: $\sigma_\rho = 70ft$, $\sigma_\theta = 1^\circ$, $\sigma_\phi = 1^\circ$.

However, the intruder states (position, velocity, acceleration) are all calculated in Cartesian coordinates. Therefore, the spherical measurements need to be converted to Cartesian states. These can be transformed using the following equation:

$$\mathbf{R}_{\text{cart}} = \mathbf{J} \times \mathbf{R}_{\text{sph}} \times \mathbf{J}' \quad (24)$$

where:

- \mathbf{R}_{cart} are the measurement noise covariances for each model - cartesian coordinates.
- \mathbf{R}_{sph} are the measurement noise covariances for each model - spherical coordinates.
- \mathbf{J} is the Jacobian, calculated as shown in [19].

C. Simulation Steps

The idea is to generate the intruder aircraft random trajectory using the outputs from the encounter model. The initial conditions and control are scalars (velocity, linear acceleration, turn rate, and the vertical velocity), so we need to provide a initial position and direction in relation to our own aircraft.

The initial position of the intruder aircraft is randomized on the surface of an “encounter cylinder” centered on the own

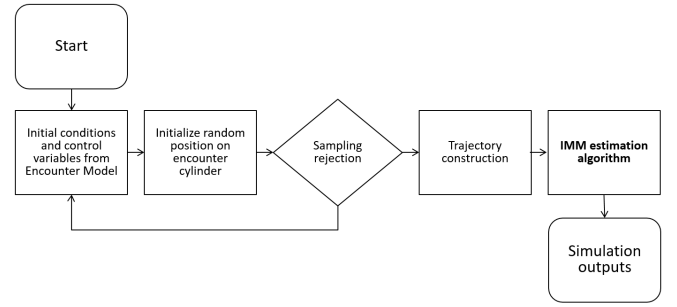


Fig. 7: Simulation Structure

aircraft, at a random heading angle. The dimensions of the cylinder is given by the minimum radar range [17] and the maximum height difference at which an “encounter” have to be considered [6]. The surface area of each top, bottom or side will give the proportion of encounters originated at that surface. We apply sampling rejection for the initial position conjugated with the initial control variables from the encounter model. If the intruder is not in an inward trajectory from the surface, we repeat the initialization until we get a suitable encounter.

Using the encounter model output, the intruder trajectory is built using point-mass kinematics to update the aircraft states. The trajectory is then inserted into the IMM estimation algorithm, using the encounter model outputs as inputs for the true intruder trajectory. Finally, we get the simulation outputs for analysis as shown in Figure 7.

In this way, the IMM estimator is being fed with measurements that are effectively perfect. The usefulness of this idealistic exercise is discussed in Section II-D, IMM Estimation Error Sources.

Along the simulation we need some additional flags for separating the trajectories into which ones we are interested, such as WCT violation and exit from the field of regard.

D. Results

In this subsection we have first an example of a particular trajectory, and then a Monte Carlo run to analyze the general performance of the algorithm. In both cases, the simulations were done following the flowchart in Figure 7.

For all the different encounters simulated, the own aircraft was assumed to have a linear trajectory with constant velocity of 200 kt (the upper bound aircraft speed in lower altitude regardless of maneuverability [6]), while the generated trajectory for the intruder aircraft is randomly generated by the encounter model. Each of the trajectories were simulated according to the following conditions:

- Own aircraft: linear trajectory, constant velocity of 200 kt
- Intruder aircraft: randomly generated by the encounter model
- Simulation time: 60s / sample rate: 1Hz
- With standard sensor noise (Section III-B) and zero sensor noise

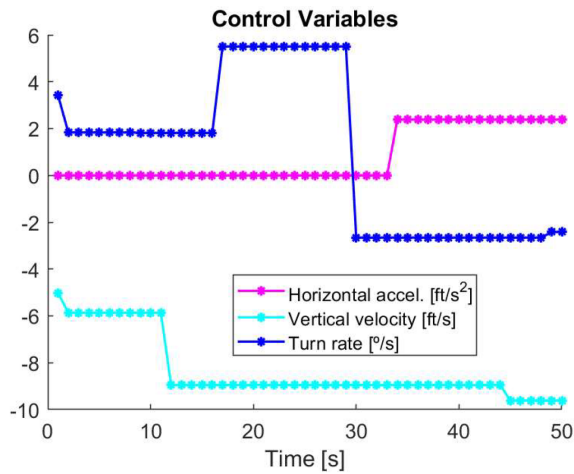


Fig. 8: Control variables for the simulation

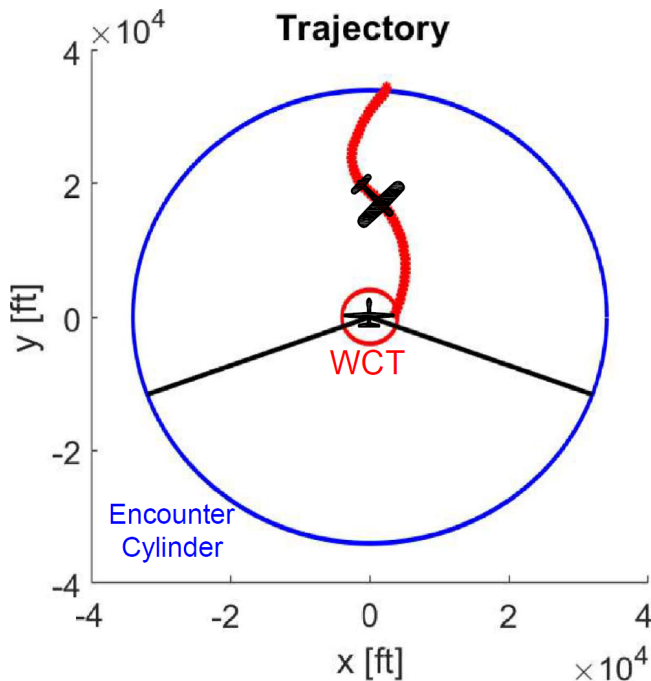


Fig. 9: Encounter trajectory

- With and without the field of regard requirements

1) *Single Maneuvering Trajectory Example:* To represent a complex scenario, we chose a trajectory in which we have all control variables non-zero as shown in Figure 8 for this simulation. The trajectory throughout the encounter cylinder is shown in Figure 9 with both cylinders shown; the encounter cylinder (blue) and the WCT (red). The encounter cylinder is assumed to have a ± 3000 ft height. Treating the radar only intruder as co-altitude for alerting when it is estimated to be within 3000 ft vertically is one acceptable mean of meeting the DAA MOPS requirements [6]. The radius of the cylinder is 5.4 NM radius, the minimum Radar Declaration Range (RDR) in clean air for a small intruder in the head-on direction [17].

For each time step, the horizontal CPA is estimated and

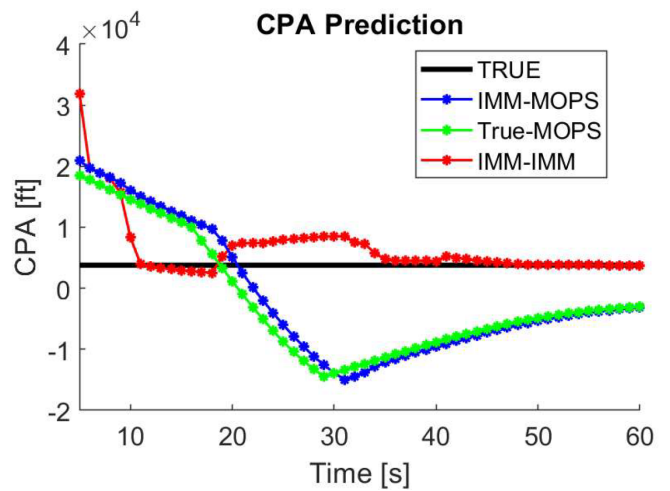


Fig. 10: CPA estimation - Zero sensor noise

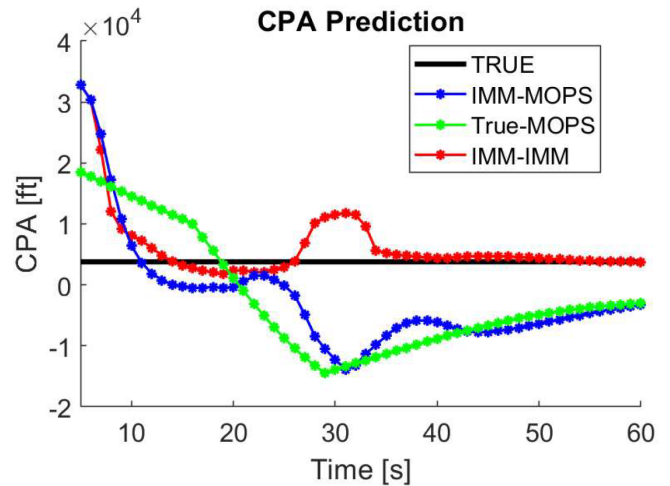


Fig. 11: CPA estimation with sensor noise

after the simulation is finished we plotted a graph comparing the CPA estimation using the new method against the MOPS calculation. The CPA estimation error for this trajectory is shown in Figure 10 and Figure 11. In the first one we can take a look at the results with zero sensor noise (as in previous work). For the second we can see how the realistic sensor affect the results, increasing the difference between the IMM-MOPS and the True-MOPS (with *true trajectory data*). It is important to make clear the difference between the states estimates and the prediction method, for example in the IMM-MOPS, we are using the IMM for estimation and the MOPS equations for prediction. As expected, with an additional error source (as discussed in Section II-D) the difference of the calculated hazard states will be greater due to sensor noise. When comparing to the new IMM Prediction method, it shows a better prediction than the MOPS CPA formula, even using *True data*, since the formula this MOPS formula extrapolates linearly an intruder trajectory.

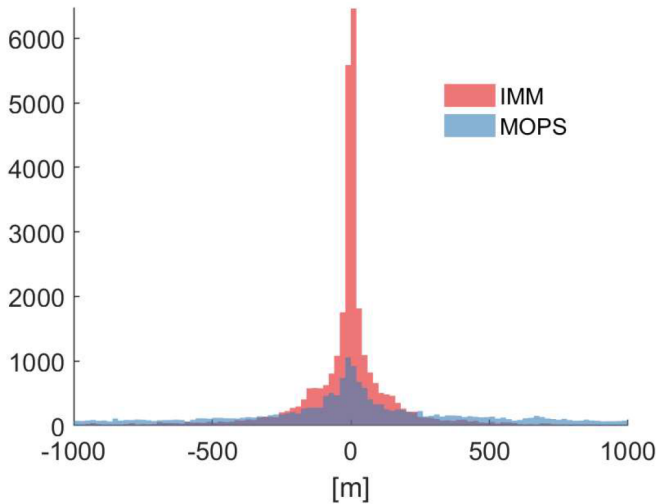


Fig. 12: CPA position error histogram

2) *Monte Carlo Results:* In order to compare the general performance of the IMM prediction estimation method, we ran 10^4 different encounters comparing it and the DAA MOPS calculation against the True CPA value.

First we present a histogram of all the position error values in the CPA estimation (concatenated for x and y positions) in Figure 12. We can observe here that the results from the IMM have a smaller deviation than using the DAA MOPS calculation.

Following we present a scatterplot of the same values in Figure 13. It is evident from this latest figure that the results from the IMM Prediction are closer to the origin, around the region of the True CPA. It is interesting to note some of the dots aligned in almost straight lines, which are all different timesteps in the same trajectory simulation.

As the estimators get more measurements, the CPA error estimation decreases as expected, moving closer to the center of the scatterplot. Also, the estimation errors are considerably reduced when using the IMM Prediction method when compared to the MOPS calculation. An additional analysis was done for both situations previously described for any encounter trajectories (including trajectories generated outside the FOR region). These trajectories include the ones that the intruder aircraft is overtaking the own aircraft and were previously considered to be among the worst-case scenario. The results showed an average prediction error 8% higher than the results previously shown.

IV. CONCLUSION

We used an encounter model to generate realistic intruder trajectories, including nonlinear intruder maneuvers, to estimate hazardous encounters for the UAS DAA problem. The intruder dynamics estimation was performed using multiple models to track the maneuvering intruder aircraft. By developing a new method to estimate hazard states (horizontal CPA, τ and vertical separation) based on the IMM prediction, we showed how this can be useful in reducing the estimation

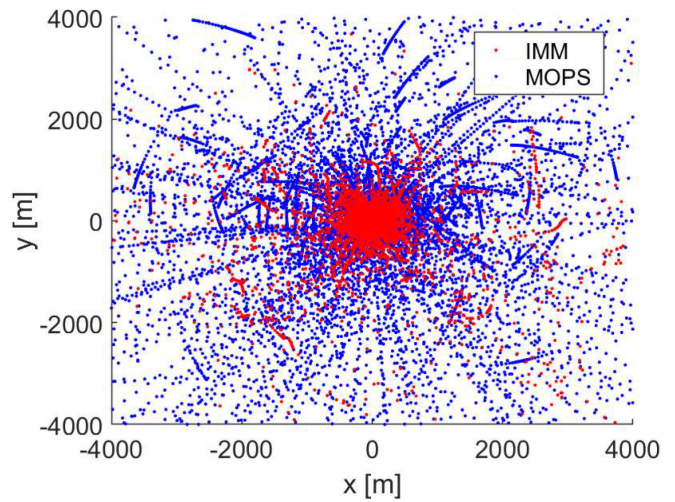


Fig. 13: CPA position error scatterplot

errors for a given sensor, even when compared to *true data*. We first examined an encounter example, then we accomplished a Monte Carlo analysis of hazardous encounters. The results showed our new IMM method for estimating horizontal CPA was a significant improvement over methods that linearly extrapolate intruder trajectories, while also considering the MOPS requirements for field of regard. Future work should include a safety evaluation based on probabilities of loss of well clear (and NMAC). Another possible area of interest for future work is the study of the maneuvering trajectories in which the intruder exits and/or reenters the FOR region.

ACKNOWLEDGMENT

This work is supported by the Brazilian agency Capes through a scholarship from Ciencia sem Fronteiras (Science without Borders) program / Process No. 99999.012923/2013-03.

REFERENCES

- [1] Federal Aviation Administration, "Integration of Civil Unmanned Aircraft Systems (UAS) in the National Airspace System (NAS) Roadmap," Washington, DC, Nov 2013.
- [2] M. Edwards, "A safety driven approach to the development of an airborne sense and avoid system," in *Infotech@Aerospace 2012*. Garden Grove, CA: American Institute of Aeronautics and Astronautics (AIAA), Jun 2012, pp. 1–12.
- [3] M. B. Jamoom, A. Canolla, B. Pervan, and M. Joerger, "Unmanned aircraft system sense and avoid integrity: Intruder linear accelerations and analysis," *Journal of Aerospace Information Systems*, vol. 14, no. 1, pp. 53–67, Jan 2017.
- [4] A. C. Canolla, M. B. Jamoom, and B. Pervan, "Unmanned aircraft systems detect and avoid sensor hybrid estimation error analysis," in *17th AIAA Aviation Technology, Integration, and Operations Conference*. American Institute of Aeronautics and Astronautics, Jun 2017.
- [5] —, "Interactive multiple model hazard states prediction for unmanned aircraft systems (UAS) detect and avoid (DAA)," in *2018 AIAA Information Systems-AIAA Infotech @ Aerospace*. American Institute of Aeronautics and Astronautics, Jan 2018.
- [6] RTCA SC-228; DO-365, "Minimum Operational Performance Standards (MOPS) for Detect and Avoid (DAA) Systems," Washington, DC, May 2017.
- [7] X. Yu and Y. Zhang, "Sense and avoid technologies with applications to unmanned aircraft systems: Review and prospects," *Progress in Aerospace Sciences*, vol. 74, pp. 152–166, Apr 2015.
- [8] A. D. Zeitlin, "Sense & avoid capability development challenges," *IEEE Aerospace and Electronic Systems Magazine*, vol. 25, no. 10, pp. 27–32, Oct 2010.
- [9] S. P. Cook, D. Brooks, R. Cole, D. Hackenberg, and V. Raska, "Defining well clear for unmanned aircraft systems," in *AIAA Infotech @ Aerospace*. Kissimmee, FL: American Institute of Aeronautics and Astronautics (AIAA), Jan 2015, pp. 1–20.
- [10] Federal Aviation Administration, "Sense and Avoid (SAA) for Unmanned Aircraft Systems (UAS), SAA Workshop Second Caucus Report," SAA Workshop Second Caucus Report, Jan 2013.
- [11] E. Mazor, A. Averbuch, Y. Bar-Shalom, and J. Dayan, "Interacting multiple model methods in target tracking: a survey," *IEEE Transactions on Aerospace and Electronic Systems*, vol. 34, no. 1, pp. 103–123, 1998.
- [12] Y. Bar-Shalom, X. R. Li, and T. Kirubarajan, *Estimation with Applications to Tracking and Navigation: Theory Algorithms and Software*. Wiley-Interscience, 2008.
- [13] I. Hwang, H. Balakrishnan, and C. Tomlin, "Performance analysis of hybrid estimation algorithms," in *42nd IEEE International Conference on Decision and Control*. IEEE, Dec 2003.
- [14] X. Li and Y. Bar-Shalom, "Performance prediction of the interacting multiple model algorithm," *IEEE Transactions on Aerospace and Electronic Systems*, vol. 29, no. 3, pp. 755–771, Jul 1993.
- [15] Z. Radosavljevi, "Determination of the transition probabilities for the interacting multiple model probabilistic data association estimator," *Scientific Technical Review*, vol. LVII, no. 2, pp. 31–37, 2007.
- [16] M. B. Jamoom, M. Joerger, and B. Pervan, "Sense and Avoid for Unmanned Aircraft Systems: Ensuring Integrity and Continuity for Three Dimensional Intruder Trajectories," in *Institute of Navigation GNSS+*, Tampa, FL, Sep 2015.
- [17] RTCA SC-228; DO-366, "Minimum Operational Performance Standards (MOPS) for Air-to-Air Radar for Traffic Surveillance," Washington, DC, May 2017.
- [18] M. J. Kochenderfer, J. K. Kuchar, L. P. Espindle, and J. D. Griffith, "Uncorrelated Encounter Model of the National Airspace System," Massachusetts Institute of Technology, Lincoln Laboratory, Project Report ATC-345, 2008.
- [19] M. B. Jamoom, "Unmanned aircraft system sense and avoid integrity and continuity," Ph.D. dissertation, Illinois Institute of Technology, May 2016.